

# Design and Fabrication of a High-Strength Hydrogel with Ideally Homogeneous Network Structure from Tetrahedron-like Macromonomers

Takamasa Sakai,<sup>\*,†</sup> Takuro Matsunaga,<sup>‡</sup> Yuji Yamamoto,<sup>§</sup> Chika Ito,<sup>§</sup> Ryo Yoshida,<sup>||</sup> Shigeki Suzuki,<sup>⊥</sup> Nobuo Sasaki,<sup>#</sup> Mitsuhiro Shibayama,<sup>‡</sup> and Ung-il Chung<sup>\*,†</sup>

Department of Bioengineering, School of Engineering, The University of Tokyo, 7-3-1 Hongo, Bunkyo-ku, Tokyo 113-8656, Japan; The Institute for Solid State Physics, The University of Tokyo, 5-1-5 Kashiwanoha, Kashiwa 277-8581, Japan; NOF Corporation, 3-3 Chidori-cho, Kawasaki-ku, Kawasaki, Kanagawa 210-0865, Japan; Department of Materials Engineering, Graduate School of Engineering, The University of Tokyo, 7-3-1 Hongo, Bunkyo-ku, Tokyo 113-8656, Japan; NEXT 21, 3-38-1 Hongo, Bunkyo-ku, Tokyo 113-0033, Japan; and Department of Veterinary Medical Sciences, Graduate School of Agricultural and Life Sciences, The University of Tokyo, 1-1-1 Yayoi, Bunkyo-ku, Tokyo 113-8657, Japan

Received March 4, 2008; Revised Manuscript Received May 8, 2008

**ABSTRACT:** As a new class of high-strength hydrogels, we designed a tetra-PEG gel by combining two symmetrical tetrahedron-like macromonomers of the same size. Because the nanostructural unit of the gel network was defined by the length of the tetrahedral PEG arm, the gel had a homogeneous structure and resultant high mechanical strength comparable to that of native articular cartilage. Furthermore, since the gel was formed by mixing two biocompatible macromonomer solutions, the gelation reaction itself and the resultant gel were also biocompatible. The breaking strength had local maxima at the overlap concentration of the macromonomers ( $C^*$ ) and at  $2C^*$ . Dynamic light scattering measurement indicated the near absence of inhomogeneities in the network at  $C^*$ . Thus, we successfully designed and fabricated a high-strength hydrogel by controlling the homogeneity of network structure for the first time, which will lead to multiplied effects, i.e., contributing to the understanding of ideal networks, providing a universal strategy for designing high-strength gels, and opening up the biomedical application of hydrogels.

## Introduction

Hydrogels are defined as 3D polymer networks, in which aqueous solution exists as a solvent. Most hydrogels are composed of 90% water. Initially, taking advantage of their high water absorption and retention properties, hydrogels were applied to diapers, contact lenses, drug reservoirs, etc. After the volume-phase transition behavior was discovered by Tanaka et al. in 1978,<sup>1</sup> a variety of functional materials such as sensors and actuators were developed on the basis of their stimulus responsiveness.<sup>2–6</sup> Despite these unique characteristics, practical applications of hydrogels, especially as structural materials, are restricted because of their low mechanical strength, which results from the microinhomogeneities of polymeric topological structure created by cross-linking.<sup>7</sup> The inhomogeneities are categorized into spatial, topological, connectivity, and motility inhomogeneities.<sup>8</sup> As the networks cannot behave cooperatively due to these inhomogeneities, they begin to break from the weakest link, thus reducing the whole mechanical strength. In order to achieve the cooperativeness, various types of hydrogels with unique network structure have been developed, e.g., a topological gel with sliding cross-linkers,<sup>9</sup> a nanocomposite gel synthesized by polymerizing with dispersed clay disks,<sup>10</sup> and a

double-network gel containing two types of independent networks.<sup>11</sup> Although these gels have unprecedented mechanical properties because of their cooperativeness, considering applications as a biomaterial, there were concerns over difficult fabrication process and toxic residual monomers. In contrast to these unique gels, other researchers have pursued the ideally homogeneous network structure for a long time. The ideally homogeneous gel network is expected to have high mechanical properties including modulus and breaking strength.<sup>12</sup>

In order to obtain an ideal gel network along with its resultant high mechanical properties, many attempts were made, including gelation by physical cross-linking, gelation from macromonomers,<sup>13</sup> gelation from polymers by  $\gamma$ -ray irradiation,<sup>14</sup> etc. Homogeneity could be relatively easily obtained by physical cross-linking. However, the homogeneity cannot be controlled strictly in physical gels because cross-linking occurs at random. In addition, physical cross-linking was generally weak, and the resulting physical gels became soft and weak. Gelation from macromonomers seemed more promising than the others because the detailed network structure was controllable by designing constitutional units, and the gelation process was predicted easily by the tree approximation of Flory and the cascade model of Gordon.<sup>15,16</sup> He et al. reported the synthesis of jungle-gym-type polyimide organogels using trifunctional cross-linkers and telechelic rigid aromatic oligomers as backbones, which had a high compression modulus.<sup>17</sup> As for hydrogels, there were numerous studies to obtain the homogeneous biocompatible hydrogels.<sup>18–21</sup> To the best of our knowledge, however, no hydrogels formed from macromonomers have compressive strength, reaching a megapascal range; most of the papers did not discuss the compressive strength, which is one of the most important parameters for practical use. The fragility may come from microinhomogeneity of the network structure.

\* To whom correspondence should be addressed: Ph +81-3-5841-8199, +81-3-5841-8843; Fax +81-3-5841-1510; e-mail sakai@cnbi.t.u-tokyo.ac.jp, tei@bioeng.t.u-tokyo.ac.jp.

<sup>†</sup> Department of Bioengineering, School of Engineering, The University of Tokyo.

<sup>‡</sup> The Institute for Solid State Physics, The University of Tokyo.

<sup>§</sup> NOF Corporation.

<sup>||</sup> Department of Materials Engineering, Graduate School of Engineering, The University of Tokyo.

<sup>⊥</sup> NEXT 21.

<sup>#</sup> Department of Veterinary Medical Sciences, Graduate School of Agricultural and Life Sciences, The University of Tokyo.

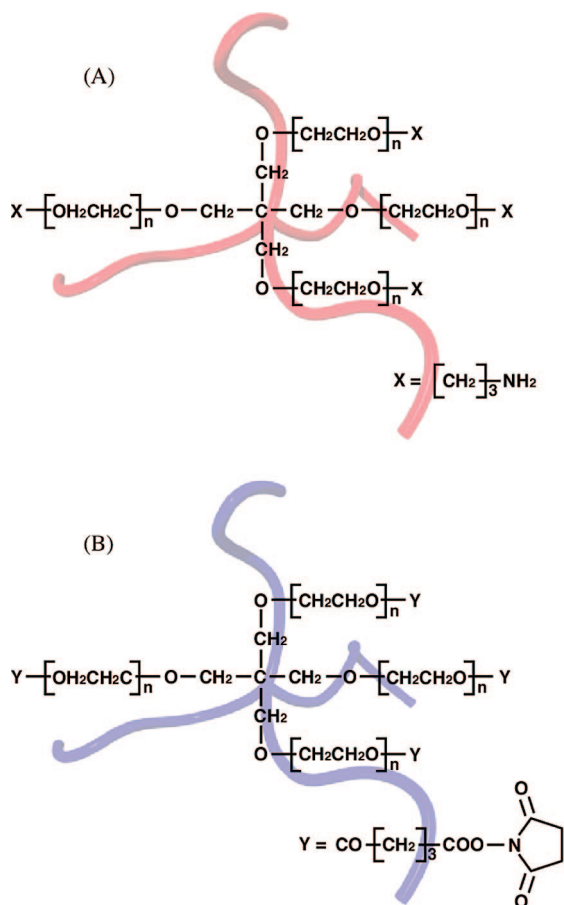


**Figure 1.** Molecular structures of TAPEG (A) and TNPEG (B).

Focusing the spotlight on constitutional unit of the network, most of gels from macromonomers were formed from asymmetrical components such as multifunctional cross-linkers and telechelic polymers. These asymmetrical combinations should give the network a high degree of freedom, allowing various microstructure including loops and defects. These various microinhomogeneities deprive network of the cooperativeness, resulting in weakening the gels.

Here, we show the new strategy for forming a homogeneous network by decreasing the degree of freedom of the micronetwork structure. We formed the gel by combining two well-defined symmetrical tetrahedron-like macromonomers of the same size (Figure 1). As each macromonomer has four end-linking groups reacting with each other, these two macromonomers must connect alternately with avoiding the self-reaction. This gelation process is simple A–B type reaction going along with Flory's classical theory; the gel was formed by mixing two macromonomer solutions within several minutes. We named this hydrogel tetra-PEG gel. The constitutional macromonomers and the reaction were biocompatible, and the compressive strength of resulting gel was in a megapascal range which was much superior to those of agarose gels or acrylamide gels having the same network concentrations (Figure 2). We discuss the relation between the mechanical properties and homogeneity of the network structure.

## Experimental Section

**Preparation of Tetrahydroxyl-Terminated PEG (THPEG).** THPEGs were synthesized by successive anionic polymerization reaction of ethylene oxide from sodium alkoxide of pentaerythritol. The molecular weight was estimated from the hydroxyl value. The hydroxyl value was determined by an esterification reaction with phthalic anhydride in a pyridine solution; subsequently, excess of

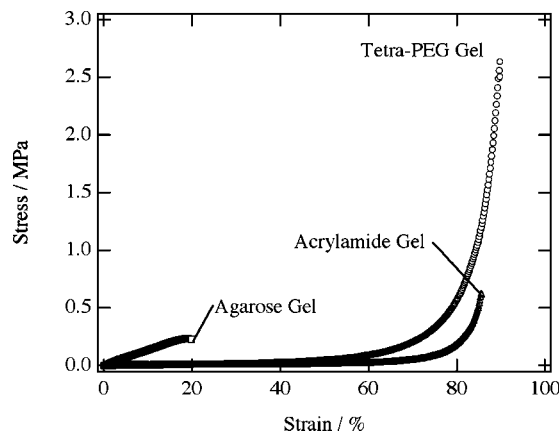


**Figure 2.** Stress–strain curves of agarose gel (square), acrylamide gel (triangle), and tetra-PEG gel (circle).

phthalic acid was estimated by alkaline titration using sodium hydrate solution according to a method (JIS K 1557) filed in Japan Industrial Standards (JIS).

**Preparation of Tetraamine-Terminated PEG (TAPEG).** 100 g of THPEG was dissolved in 100 g of KOH aqueous solution. Then, acrylonitrile was added, followed by reaction for 4 h. After neutralization, the product was extracted from the aqueous solution into chloroform and then concentrated by evaporation. The extract was purified by a repeated crystallization using ethyl acetate and hexane; via drying in vacuum, the tetranitrile-terminated PEG was recovered. 90 g of the tetranitrile-terminated PEG dissolved in 360 g of toluene was hydrated with 9 g of Ni/carbon catalysis under NH<sub>3</sub> and H<sub>2</sub> pressure. The toluene solution was filtrated and crystallized by adding an excess amount of hexane. After filtration and drying, TAPEG was obtained. Molecular weight (*M<sub>w</sub>*) was estimated from the hydroxyl value of raw THPEGs. The molecular weight distribution (MWD) was measured by gel permeation chromatography (GPC) (LC-10Avp, Shimadzu). The activity of the functional group was estimated using NMR.

**Preparation of Tetra-NHS-Glutarate-Terminated PEG (TNPEG).** 100 g of THPEG were dissolved in 150 g of toluene. After dehydration, 6.9 g of glutaric anhydride and sodium acetate (0.5 g) were added to the solution. The reaction was performed under reflux condition (~110 °C) for 12 h. The reaction solution containing tetraglutaric acid-terminated PEG was cooled to 40 °C. Then, 13.8 g of *N*-hydroxysuccinimide and 17 g of *N,N'*-dicyclohexylcarbodiimide were added and reacted at 40 °C for 3 h. The mixture was purified by a repeated crystallization process from a solvent system comprised of toluene, ethyl acetate, and hexane. The crystalline precipitate was dried in vacuum, and TNPEG was recovered. The *M<sub>w</sub>*, MWD, and activity of the functional group were measured by the same method as TAPEG.

**Viscometric Measurement of TAPEG and TNPEG Aqueous Solution.** Constant amounts of TAPEG and TNPEG ranging from 50 to 3000 mg were resolved in 20 mL of water. The relative viscosity of the solutions was measured with a rheometer (MCR501, Anton Paar), using the concentric double cylinder at a constant shear rate of 100 s<sup>-1</sup>. All experiments were carried out at 25 °C.

**DLS Measurement of TAPEG and TNPEG.** TAPEG and TNPEG (100 mg) were resolved into 10 mL of water. For resultant solutions, dynamic light scattering (DLS) measurements were taken at a 90° angle by using a static/dynamic compact goniometer (SLS/DLS-5000, ALV). A He–Ne laser with a power of 22 mW emitting a polarized light at  $\lambda = 632.8$  nm was used as the incident beam. All the measurements were carried out at 20 °C. The characteristic decay time distribution function,  $G(\Gamma^{-1})$ , was obtained from  $g^{(2)}(\tau)$  with an inverse Laplace transform program (a constrained regularization program, CONTIN provided by ALV).

**TRDLS Measurement of Tetra-PEG Gel.** TAPEG and TNPEG (600 mg) were resolved into 0.1 M phosphate buffer (10 mL), pH 7.4 and 7.2, respectively. After mixing two solutions in a 10 mm

**Table 1. Molecular Weight ( $M_w$ ) Estimated from Hydroxyl Value, Polydispersity ( $M_w/M_n$ ) Measured by Gel Permeation Chromatography, and Activity of the Functional Groups Estimated by NMR**

properties	TAPEG	TNPEG
molecular weight ( $M_w$ )	9617	11 091
polydispersity ( $M_w/M_n$ )	1.05	1.01
functionality of end group (%)	92.7	92.9

Pyrex test tube, DLS measurements were taken at an interval of 30 s at a 90° angle by using a static/dynamic compact goniometer (SLS/DLS-5000, ALV). All the measurements were carried out at 20 °C.

**Compression Test of Agarose Gel and Acrylamide Gel.** Agarose (600 mg) was dissolved into 10 mL of water at 85 °C. The solution was poured into an acryl cylinder that was 15 mm in diameter and 7.5 mm in height. Then, agarose gel was obtained by cooling it at room temperature for 2 h. Acrylamide (600 mg) and  $N,N'$ -methylenebis(acrylamide) (9.2 mg) (one cross-linker per 10 000 Da) were resolved into 10 mL of water at room temperature. Then, 50  $\mu$ L of aqueous solution of ammonium persulfate (100 mg/mL) and 6  $\mu$ L of  $N,N,N',N'$ -tetramethylethylenediamine were added to the solution. The acrylamide gel was synthesized in an acryl cylinder that was 15 mm in diameter and 7.5 mm in height. The compression test was carried out using a mechanical testing apparatus (INSTRON 3365, Instron Corp.) at a velocity of 0.75 mm/min.

**Compression Test of Tetra-PEG Gel.** Constant amounts of TAPEG and TNPEG ranging from 400 to 1600 mg were resolved into 0.1 M phosphate buffer (10 mL), pH 7.4 and pH 7.2, respectively. Two equal amounts of polymer solutions were mixed under room temperature, and the gelation was initiated in an acryl cylinder that was 15 mm in diameter and 7.5 mm in height for 2 h. The compression test was carried out using a mechanical testing apparatus (INSTRON 3365, Instron Corp.) at a velocity of 0.75 mm/min. More than 10 samples were tested for each network concentration.

**Stoichiometric Study of Tetra-PEG Gel.** Constant total amounts of TAPEG and TNPEG (total amount of precursors = 600 mg) with a TAPEG to TNPEG ratio ranging from 0.33 to 3.0 were dissolved into 0.1 M phosphate buffer (10 mL), pH 7.2 and pH 7.4, respectively. Two equal volumes of polymer solutions were mixed under room temperature, and the gelation was initiated in an acryl cylinder that was 15 mm in diameter and 7.5 mm in height for 2 h. The compression test was carried out using a mechanical testing apparatus (INSTRON 3365, Instron Corp.) at a velocity of 0.75 mm/min.

**DLS Measurement of Tetra-PEG Gel.** Tetra-PEG gels containing polymer networks ranging from 20 to 140 mg/mL were prepared by the above-mentioned method in 10 mm Pyrex test tubes. DLS measurements were performed at a 90° angle using SLS/DLS-5000 at 20 °C. In order to obtain the ensemble average, the intensity–time correlation function,  $g^{(2)}(\tau)$ , was measured at 100 different sample positions.

## Results and Discussion

**Design and Fabrication of Tetra-PEG Gel.** In order to form a homogeneous network structure, we designed a novel hydrogel synthesized in situ by mixing solutions of two kinds of macromonomers with different reactive terminal groups. As constitutional units, two types of 4-armed poly(ethylene glycol) (PEG) were synthesized with a tetrahedron-like structure (tetraamine-terminated PEG (TAPEG) and tetra-NHS-glutarate-terminated PEG (TNPEG)). The terminal groups of TAPEG and TNPEG were propylamine and succinimidyl glutarate, respectively (Figure 1a,b, Table 1). TAPEG and TNPEG were monodisperse, and the  $M_w$  was approximately 10 000 Da; the molecular weight of one arm was about 2500 Da (Table 1). Four arms had a fixed bond angle (109.47°), and the motility of the arms was likely restricted by steric repulsion. Thus, the

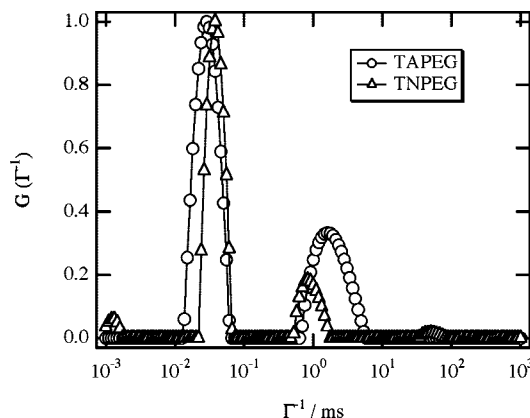


**Figure 3.** Characteristic distribution function,  $G(\Gamma^{-1})$ , for the TAPEG (circle) and TNPEG (triangle) measured by dynamic light scattering. The characteristic distribution function was obtained from the intensity–time correlation function.

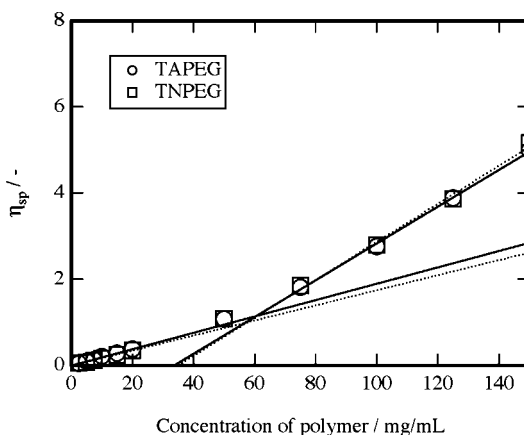


**Figure 4.** Relative viscosity of the solutions measured by a rheometer as a function of polymer concentration [TAPEG] (circle and solid line) and [TNPEG] (square and broken line). From the point at the intersection of the fitting lines of higher concentration and lower concentration, the overlap concentration ( $C^*$ ) was estimated.

shape of the macromonomer was assumed to be tetrahedron-like, having a spatial symmetry capable of filling the 3D space. Figure 3 shows the characteristic distribution function,  $G(\Gamma^{-1})$ , for the TAPEG and TNPEG measured by DLS. Note that there are two modes, i.e., fast and slow modes. The fast mode corresponds to the translational diffusion of individual TAPEG or TNPEG chains. On the other hand, the slow mode appearing between  $\Gamma^{-1} = 10^0$  and  $10^1$  ms indicates that some polymer chains are clustered, as are often observed in water-soluble polymers.<sup>22</sup> Although the slow mode looks comparable to the fast mode, it is emphasized by the factor of the sixth power of the size ratio of the individual polymer chains to the clusters, i.e.,  $(R_{h,chain}/R_{h,cluster})^6$  due to the nature of scattering, i.e., the scattering intensity being proportional to the sixth power of the size of the scatterers. Here,  $R_h$  is the hydrodynamic radius. In our case, the cluster fraction is of the order of a few percent at most. Hence, this contribution can be neglected in this work. The values of  $R_h$  for the TAPEG and TNPEG were evaluated to be 2.42 and 2.85 nm, respectively.<sup>23</sup>

Figure 4 shows the specific viscosity of the solutions measured by a rheometer as a function of polymer concentration [TAPEG] (circle) and [TNPEG] (square). From the crossover of the two straight lines, the overlap concentrations ( $C^*$ ) of the macromonomers were estimated to 60 mg/mL, and the hydrodynamic radius calculated from the intrinsic viscosity using the Flory–Fox equation was 3.8 nm. The simulation result showed



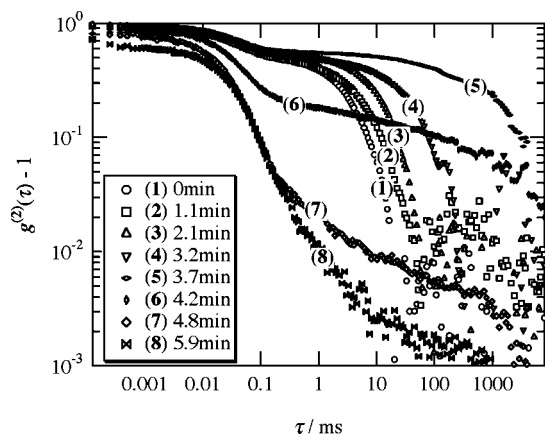


**Figure 5.** Time evolution of ICFs for tetra-PEG (60 mg/mL) in gelation process.

that the conformation of the star polymer depends on the arm length; when the polymer chain is short enough to be affected by self-avoiding condition, the chain take more elongated conformation than random coil.<sup>24</sup> Compared with the radius calculated under the assumption of random coil (3.45 nm), each arm has elongated conformation compared with random coil. When these two polymer solutions were mixed under the biological pH, amide bonds were formed between amino groups and succinimidyl ester groups, forming a network structure.

The time course of gelation can be monitored by the time-resolved DLS measurement (TRDLS). Figure 5 is a typical example showing time course of  $G(\Gamma^{-1})$ s of tetra-PEG gel during gelation process. In the cases of curves 1–5, there appeared two shoulders in  $G(\Gamma^{-1})$ . The first shoulder (the fast mode) corresponds to the translational diffusion of individual polymer chains and/or corrective diffusion, while the second shoulder (the slow mode) does to the translational diffusion of clusters. The characteristic time of the slow mode disappear when an infinite cluster is formed. In other words, the slow mode disappears when a sol–gel transition occurs as a result of divergence of the characteristic time for the slow mode. Thus, the gelation time was estimated to be ca. 4 min. The important message here is that gelation takes place in a few minutes. As this reaction is a simple polymer-to-polymer one, it can be performed in situ, with no toxic residual monomers. The dissociating succinimidyl group, which is a citric acid derivative, can be easily metabolized by the citric cycle.<sup>25</sup>

**Influence of Macromonomer Concentration on Mechanical Properties.** In order to investigate the breaking strength of tetra-PEG gel, we performed the compression test for gels having stoichiometric amounts of TAPEG and TNPEG. Figure 6 shows the mean breaking strength and breaking strain obtained from the stress–strain curve. There was a good correlation between the breaking stress and breaking strain because the compression stress increased dramatically in the larger strain region (Figure 2). The maximum breaking stress of tetra-PEG gel was 9.6 MPa at 120 mg/mL. This value was extremely high, surpassing that of conventional hydrogels (several tens to hundreds of kilopascals), and was comparable to native articular cartilage (approximately 6–10 MPa). As seen in Figure 6, the breaking stress and breaking strain had two peculiar peaks unlike conventional gels. This unique mechanical property could be interpreted by using  $C^*$  as follows. The network with  $[\text{Net}] = 40$  mg/mL was weak because the  $[\text{Net}]$  was below  $C^*$ , leading to the formation of an underdeveloped network with defects such as clusters and dangling chains. When  $[\text{Net}]$  became  $C^*$  (60 mg/mL), as macromonomers were perfectly packed in the solution, a homogeneous structure was obtained, giving the first

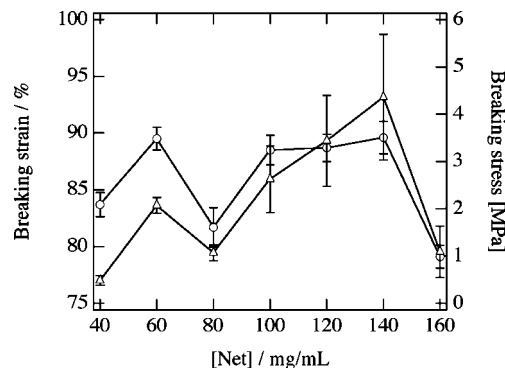


**Figure 6.** Network concentration dependence of breaking strain (circle, left axis) and breaking stress (triangle, right axis).

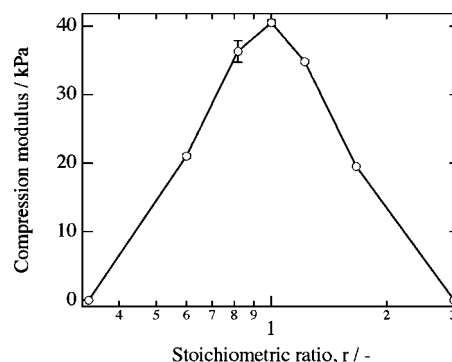


**Figure 7.** Dependence of compression modulus on stoichiometric ratio of two macromonomers. Total network concentration was kept at  $C^*$  (60 mg/mL).

peak. Then, both the breaking stress and breaking strain decreased dramatically at  $[\text{Net}] = 70$  and  $80$  mg/mL. This suggested that an excess of polymers introduced defects into the gel network. However, when  $[\text{Net}]$  was increased to  $90$  mg/mL, both the breaking stress and breaking strain began to increase again. At  $[\text{Net}] = 120$  and  $140$  mg/mL, the second peak of the breaking stress and breaking strain appeared. Because these values were equal or close to  $2C^*$ , the formation of another homogeneous structure, i.e., the double-network structure, was indicated. The network formed here was probably not a real double-network structure but pseudo one; an apparent interpenetrating network existed, but all building blocks belonged to one network. When  $[\text{Net}]$  became  $160$  mg/mL, breaking stress and breaking strain decreased again, indicating that defects were introduced into the network again.

In order to investigate the effect of the stoichiometry of two macromonomers on mechanical properties, we measured the compression modulus and breaking strength at several stoichiometric ratios  $r$  with the total macromonomer concentration being equal to  $C^*$ , where  $r$  equals the molar ratio of TAPEG to TNPEG (Figures 7 and 8). The maximum value of the compression modulus and breaking strength were obtained at  $r = 1.0$ , indicating that equimolar macromonomers reacted with each other and that even a slight excess or shortage of one component weakened the gel. Furthermore, the values of the compression modulus among reciprocal  $r$ 's were almost the same; no matter which component was in excess or shortage, the reductions in the compression modulus were similar, suggesting a similarity in their network structures. This highly stoichiometrical and symmetrical gelation process is unprecedented, strongly suggesting the formation of a homogeneous network structure of tetra-PEG gel. The optimal quantity and optimal ratio of macromonomers were needed to form the homogeneous network structure.

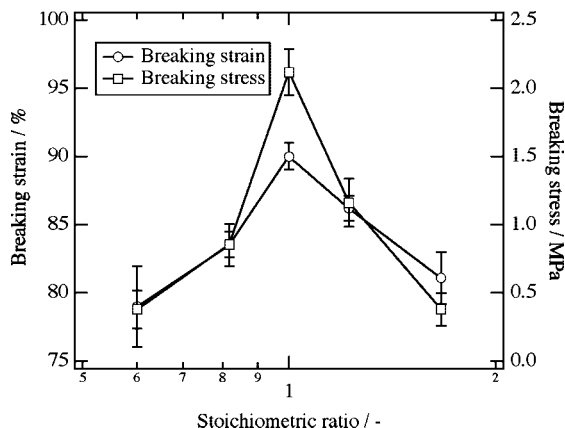


**Figure 8.** Dependence of breaking strain (circle, left axis) and breaking stress (square, right axis) on stoichiometric ratio of two macromonomers. Total network concentration was kept at  $C^*$  (60 mg/mL).

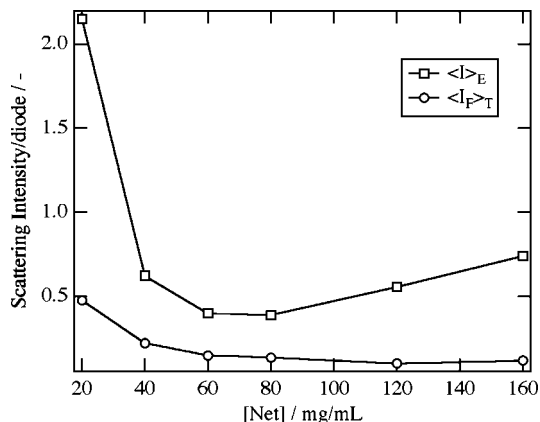


**Figure 9.** Network concentration dependence of the ensemble average  $\langle I \rangle_E$  (square) and dynamic fluctuation component  $\langle I_F \rangle_T$  (circle) of scattered light.

**Structural Analyses by DLS.** To directly analyze the network structure, we performed DLS measurement. The scattered light from gels is composed of the fluctuation component that originates from the Brownian motion of the solution and/or solute and the frozen concentration inhomogeneities introduced by cross-linking. Shibayama et al. proposed a method for decomposing the concentration fluctuation in gels into the dynamic fluctuations and the static inhomogeneities through statistical analysis of intensity–time correlation functions (ICF) obtained from different sampling points.<sup>8,26–28</sup> From the analysis, the ensemble-average scattering intensity  $\langle I \rangle_E$ , indicating the inhomogeneity of the network, and the fluctuating component  $\langle I_F \rangle_T$ , indicating the motility of the network, were obtained.

In order to investigate the influence of [Net] on the network structure, we performed DLS analysis of gels at several network concentrations ranging from 20 to 160 mg/mL. The obtained  $\langle I \rangle_E$  was very low, being comparable to that of dilute gelatin gel representative of physical gels with a homogeneous network structure. In addition, the optical transmittance of tetra-PEG gel was  $\approx 100\%$ , also indicating the homogeneous network structure.<sup>8,9</sup> Figure 9 shows the  $\langle I \rangle_E$  and  $\langle I_F \rangle_T$  as functions of [Net]. When [Net] = 20 mg/mL, both  $\langle I \rangle_E$  and  $\langle I_F \rangle_T$  were at a maximum, suggesting that the network is inhomogeneous and fluctuating. This result indicated that the constituent polymers were in short supply, resulting in the formation of an incomplete network including finite clusters.<sup>29,30</sup> When [Net] was increased to  $C^*$  (60 mg/mL), both  $\langle I \rangle_E$  and  $\langle I_F \rangle_T$  were dramatically decreased, and  $\langle I \rangle_E$  reached the minimum value. These results

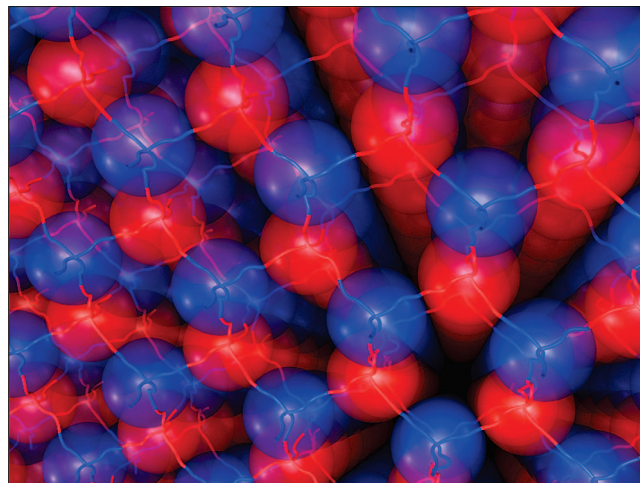


**Figure 10.** Schematic illustration of a model structure for tetra-PEG gel formed at  $C^*$ . Red and blue spheres represent TAPEG and TNPEG, respectively.

suggest that completely packed macromonomers formed a single homogeneous network. This concentration corresponds to first local maximum of compression breaking stress. When [Net] = 80 mg/mL, both  $\langle I \rangle_E$  and  $\langle I_F \rangle_T$  were almost the same as those of  $C^*$ , despite the drastic change in mechanical properties. Although the mechanism was unclear, we speculated that the existence of excess constituent polymers affected the mechanical properties. When [Net] was further increased,  $\langle I \rangle_E$  became larger because the excess network was formed. Although the network became inhomogeneous in this region,  $\langle I_F \rangle_T$  continued to decrease, reaching a minimum at [Net] = 120 mg/mL. When [Net] was further increased,  $\langle I_F \rangle_T$  became larger again. These results suggested that the network at 120 mg/mL was the most rigid. Because this concentration coincided with the second local maximum of breaking strength and was  $2C^*$ , we deduced that excess constituent polymers formed the second homogeneous network.

Taken together, we conclude that tetra-PEG gel formed at  $C^*$  has extremely homogeneous structure. From the DLS measurement, the characteristic length of the network formed at  $C^*$  was estimated to 5.3 nm, which corresponds to the double of the PEG arm length. Considering the fact that these tetrahedral macromonomers are connected alternately with small inhomogeneity at the  $C^*$  and the network had characteristic length corresponding to two arm-length, the formation of a well-defined network structure was strongly suggested (Figure 10).

## Concluding Remarks

In this study, we successfully designed and fabricated a novel homogeneous hydrogel by combining two symmetrical tetrahedron-like macromonomers of the same size. Tetra-PEG gel was prepared through a highly stoichiometrical and symmetrical gelation process. The breaking strength was extremely high, being comparable to that of native articular cartilage. Local maxima of the breaking strength and local minima of  $\langle I \rangle_E$  and  $\langle I_F \rangle_T$  were obtained at  $C^*$  and  $2C^*$ , indicating the formation of a homogeneous network structure. Judging from these data, we conclude that tetra-PEG gel has an extremely homogeneous network structure. To the best of our knowledge, this is the first successful fabrication of a homogeneous chemical hydrogel having high mechanical strength. Since the mechanical properties of ideal networks can be modified by increasing the length between cross-linking points,<sup>31</sup> we plan to further increase the mechanical properties of tetra-PEG gel by controlling the PEG arm length. Furthermore, we plan to fabricate stimuli-responsive

hydrogels using this strategy from tetrahedron-like macromonomers. High homogeneity of the network may dramatically enhance the degree and kinetics of volume change.

In addition, tetra-PEG gel may be valuable in application for practical use. For biomedical applications, hydrogels are required to meet three criteria at the same time: high mechanical properties, biocompatibility, and an easy fabrication process. Tetra-PEG gel has successfully satisfied all three criteria. First, it has attained high mechanical properties using symmetrical tetrahedron-like constitutional polymers to form an extremely homogeneous structure. Second, tetra-PEG gel uses biocompatible tetrahedron-like PEG with mutually reactive terminal groups; its gel formation reaction does not use or produce any toxic substance. Third, tetra-PEG gel can be fabricated within a few minutes through in situ gelation by simply mixing two macromonomer solutions. Because of these combined merits, we strongly believe that tetra-PEG gel and its derivatives may be useful in the biomedical field.

In conclusion, by combining symmetrical tetrahedron-like macromonomers, we successfully controlled gel network structure and the resultant mechanical properties. Tetra-PEG gel will not only be useful as a biomaterial but may also contribute to the understanding of ideal networks. Furthermore, as we may be able to apply this strategy regardless of polymer species, we believe that this strategy will have a strong impact on the field of gel research.

**Acknowledgment.** We thank Toru Hakukawa for invaluable advice on gel formation. This work was partially supported by the Ministry of Education, Science, Sports and Culture, Japan (Grant-in-Aid for Scientific Research on Priority Areas, 2006-2010, No. 18068004) and the Program for Promotion of Fundamental Studies in Health Sciences of the National Institute of Biomedical Innovation (NIBIO).

## References and Notes

- (1) Tanaka, T. *Polymer* **1979**, *20* (11), 1404–1412.
- (2) Miyata, T.; Uragami, T.; Nakamae, K. *Adv. Drug Delivery Rev.* **2002**, *54* (1), 79–98.
- (3) Nakayama, D.; Takeoka, Y.; Watanabe, M.; Kataoka, K. *Angew. Chem., Int. Ed.* **2003**, *42* (35), 4197–4200.
- (4) Osada, Y.; Okuzaki, H.; Hori, H. *Nature (London)* **1992**, *355* (6357), 242–244.
- (5) Okuzaki, H.; Kunugi, T. *J. Polym. Sci., Part B: Polym. Phys.* **1996**, *34* (10), 1747–1749.
- (6) Zrinyi, M.; Feher, J.; Filipcsei, G. *Macromolecules* **2000**, *33* (16), 5751–5753.
- (7) Shibayama, M. *Bull. Chem. Soc. Jpn.* **2006**, *79* (12), 21.
- (8) Shibayama, M. *Macromol. Chem. Phys.* **1998**, *199* (1), 1–30.
- (9) Okumura, Y.; Ito, K. *Adv. Mater.* **2001**, *13* (7), 485.
- (10) Haraguchi, K.; Takehisa, T. *Adv. Mater.* **2002**, *14* (16), 1120–1124.
- (11) Gong, J. P.; Katsuyama, Y.; Kurokawa, T.; Osada, Y. *Adv. Mater.* **2003**, *15* (14), 1155.
- (12) Mark, J. E.; Erman, B. *Rubberlike Elasticity—A Molecular Primer*; Wiley: New York, 1988.
- (13) Shibayama, M.; Takahashi, H.; Nomura, S. *Macromolecules* **1995**, *28* (20), 6860–6864.
- (14) Norisuye, T.; Masui, N.; Kida, Y.; Ikuta, D.; Kokufuta, E.; Ito, S.; Panyukov, S.; Shibayama, M. *Polymer* **2002**, *43* (19), 5289–5297.
- (15) Flory, P. J. *J. Am. Chem. Soc.* **1941**, *63*, 14.
- (16) Gordon, M. *Proc. R. Soc. London, Ser. A* **1962**, *268* (1333), 240.
- (17) He, J. H.; Machida, S.; Kishi, H.; Horie, K.; Furukawa, H.; Yokota, R. *J. Polym. Sci., Part A: Polym. Chem.* **2002**, *40* (14), 2501–2512.
- (18) Martens, P.; Anseth, K. S. *Polymer* **2000**, *41* (21), 7715–7722.
- (19) Lutolf, M. P.; Hubbell, J. A. *Biomacromolecules* **2003**, *4* (3), 713–722.
- (20) Azab, A. K.; Orkin, B.; Doviner, V.; Nissan, A.; Klein, M.; Srebnik, M.; Rubinstein, A. *J. Controlled Release* **2006**, *111* (3), 281–289.
- (21) Malkoch, M.; Vestberg, R.; Gupta, N.; Mespouille, L.; Dubois, P.; Mason, A. F.; Hedrick, J. L.; Liao, Q.; Frank, C. W.; Kingsbury, K.; Hawker, C. J. *Chem. Commun.* **2006**, (26), 2774–2776.
- (22) Shibayama, M.; Karino, T.; Okabe, S. *Polymer* **2006**, *47* (18), 6446–6456.
- (23) Matsuda, Y.; Kawata, T.; Sugihara, S.; Aoshima, S.; Sato, T. *J. Polym. Sci., Part B: Polym. Phys.* **2006**, *44* (8), 1179–1187.
- (24) Forni, A.; Ganazzoli, F.; Vacatello, M. *Macromolecules* **1997**, *30* (16), 4737–4743.
- (25) Taguchi, T.; Saito, H.; Aoki, H.; Uchida, Y.; Sakane, M.; Kobayashi, H.; Tanaka, J. *Mater. Sci. Eng. C* **2006**, *26* (1), 9–13.
- (26) Shibayama, M.; Norisuye, T.; Nomura, S. *Macromolecules* **1996**, *29* (27), 8746–8750.
- (27) Shibayama, M.; Takata, S.; Norisuye, T. *Physica A* **1998**, *249* (1–4), 245–252.
- (28) Shibayama, M.; Fujikawa, Y.; Nomura, S. *Macromolecules* **1996**, *29* (20), 6535–6540.
- (29) Norisuye, T.; Takeda, M.; Shibayama, M. *Macromolecules* **1998**, *31* (16), 5316–5322.
- (30) Herning, T.; Djabourov, M.; Leblond, J.; Takerkart, G. *Polymer* **1991**, *32* (17), 3211–3217.
- (31) Obukhov, S. P.; Rubinstein, M.; Colby, R. H. *Macromolecules* **1994**, *27* (12), 3191–3198.

MA800476X